ELSEVIER

Applied Surface Science 108 (1997) 23–32

applied surface science

An investigation of the ESD O/O^+ ratio from V_2O_5 and oxidized V

Mitch Jacoby [a,1], F.J. Northrup [a], P.C. Stair [a,*], E. Weitz [a], L.D. Marks [b]

[a] *Center for Surface Radiation Damage Studies and Department of Chemistry, Northwestern University, Evanston, IL 60208, USA*

[b] *Center for Surface Radiation Damage Studies and Department of Materials Science and Engineering, Northwestern University, Evanston, IL 60208, USA*

Received 4 December 1995; accepted 12 July 1996

Abstract

The ratio of oxygen atoms to ions (O/O^+) generated during electron stimulated desorption (ESD) from V_2O_5 and oxidized V foil has been investigated. Desorbates were probed directly with high resolution quadrupole mass spectrometry. X-ray photoelectron spectroscopy was used as an indirect probe to measure the ESD induced surface oxygen loss. Despite the number of ESD target preparation methods and experimental variations used, ESD O atoms were never detected. Accordingly, the results are presented as an upper limit to the ESD O/O^+ ratio, as determined by the neutral detection limit of the given instrumental method. The results of the mass spectral probe were an O/O^+ ratio of $\simeq 54$ (oxidized V foil), 58 ($^{18}O_2/V_2O_5$) and 160 (V_2O_5). From the XPS results (oxidized V foil) the ratio was determined to be $\simeq 4$.

1. Introduction

Stimulated desorption (known collectively as DIET; desorption induced by electronic transitions) has been the subject of considerable interest for nearly 35 years, as is evident from the ~ 1000 research papers that have been published on this topic since 1960 [1] [2]. Of the wide variety of systems investigated, the maximal valence oxides (e.g. TiO_2, V_2O_5, WO_3) gained particular attention because O^+ DIET could not be rationalized within the classic Menzel–Gomer–Redhead (MGR) model [3,4]. Specifically, the MGR model was unable to explain desorption of O^+ from a lattice of O^{2-} with a desorption threshold corresponding to excitation of a metal core level. To explain these observations, Knotek and Feibelman (KF) proposed a desorption model based on an Auger decay mechanism [5,6]. In the case of V_2O_5, the KF mechanism is as follows: the highly ionic character of V_2O_5 leaves V with no valence electrons. The highest lying V electrons are at the V(3p) level. The dominant relaxation mode following ejection of a V(3p) electron (by an incident electron beam) is an inter-atomic Auger process. The V(3p) vacancy is filled by a neighboring O(2s) electron. Energy is conserved by emission of Auger electrons from the O(2s) level. If two Auger electrons are emitted (a double Auger process), a total of three electrons will have been removed from

* Corresponding author. Tel.: +1-708-491-5266; fax: +1-708-491-7713; e-mail: pstair@nwu.edu.

[1] Environmental Analytics, Inc., Schaumburg, IL 60193, USA.

[2] Many useful references may be found in the five DIET books [2].

PII S0169-4332(96)00580-6

an O atom. O^{2-} is thus converted to O^+ and promptly desorbs due to Coulomb repulsion.

Although an O^+ desorption mechanism is provided, KF indicated that DIET from these oxides is expected to produce more neutral O than O^+ because (1) the double Auger process is uncommon (8% relative probability in Ne) and (2) formation of the initial hole at the O(2s) level favors neutral O desorption [6]. In addition, if O^+ is formed at the oxide surface, it has an appreciable probability of being neutralized and desorbing as neutral O. The O/O^+ ratio is therefore predicted to be not less than ~ 100. As with most DIET studies, investigations of V_2O_5 have generally been limited either to analysis of the species desorbing from the surface or analysis of the substrate. Further, desorbate analyses appear to have been limited to ionic species. Clearly, a more complete picture of the DIET process may be obtained through an investigation that includes the substrate and both ionic and neutral desorbates. This paper reports the results of an ESD study of V_2O_5 and oxidized V foil in which the neutral to ion stimulated desorption ratio was probed directly, through desorbate analysis, and indirectly by studying the ESD induced modifications to the substrate.

1.1. ESD of oxygen from V_2O_5

The electron beam induced depletion of oxygen from the V_2O_5 (010) single crystal surface was studied by Colpaert and coworkers [7,8]. Low energy electron diffraction (LEED) investigations indicated that V_2O_5 is transformed under electron irradiation to V_6O_{13}. Knotek and Feibelman [5,6] reported desorption threshold and ion yield measurements from V_2O_5 and V_2O_3 in the development of their desorption model. An O^+ desorption threshold was observed at the metal core ionization potential for V_2O_5 but not for V_2O_3 in agreement with the Auger decay model. Photon stimulated desorption studies on the V_2O_5 (010) surface [9] demonstrated that O^+ desorption is strongly peaked in the direction of the surface normal with a most probable kinetic energy of 4.4 eV. In addition to these reports, a series of papers on the high resolution transmission electron microscopy of V_2O_5 have appeared recently in the literature [10–13]. Experimental details and a theoretical treatment of the electron beam induced phase transition kinetics from V_2O_5 to VO by way of intermediate V oxides were presented. The nature of the intermediate oxides was found to be dependent on the electron flux. Included with these substrate analyses is a report on the dependence of the O^+ yield on time (constant current electron source) and temperature [11]. The authors conclude that a diffusion controlled desorption mechanism is operative. Thus, a survey of the V_2O_5 DIET literature indicates that electron beam induced loss of oxygen is well established. Although it is generally accepted that the stimulated desorption probability is several orders of magnitude larger for neutrals than for ions, none of the cited papers report detection of neutral desorbates.

1.2. DIET of neutrals

Due to the ease of detecting ionic desorbates relative to neutrals, the vast majority of the ESD literature (particularly before DIET II [1,2]), contains reports on the yield and kinetic energy of desorbed ionic species with little mention of neutrals. Most of the early reports on neutral ESD are based upon a kinetics model in which the neutral desorption cross-section is determined, indirectly, from measuring the time dependence of the ESD ion signal decay [14]. Although such experiments may offer reliable results, a more convincing argument can be made if both neutral and ionic desorbed species are detected, and then conclusions are drawn about their relative cross-sections or abundances. The results of the indirect measurements could be in error, for example, if the coverage was not known accurately, or if the ion yield decreased due to diffusion into the bulk or conversion to an unmonitored species. Nonetheless, the ESD O/O^+ ratio from O_2 dosed metals has been determined in this manner. From the O_2/W system, O/O^+ ratios of 10 [15] and $\simeq 20$ [16] have been reported. Redhead has reported O/O^+ ratios of $\simeq 49$ and 55 from O_2/Mo [4]. The O/O^+ ratio for V_2O_5 or O_2/V does not appear to have been reported. A wider range of ratios ($\simeq 10$–10^3) has been reported for other systems, such as the CO/CO^+ ratio from CO/W or the O/O^+ ratio from CO_2/W [14,15].

Electron stimulated desorption of neutral species has been detected directly using a variety of techniques. Mass spectrometers with modified ionizers or detectors [17,18], the direct detection of energetic

metastables [19], and the use of optical techniques to measure the emission spectra from excited species [20–22] have been employed. Laser techniques have been used in neutral ESD studies because of their high ionization efficiency and selectivity. A discussion of these methods together with recent results from the O_2/Ag system is deferred to a forthcoming paper [23].

2. Experimental

Two types of experiments were conducted in the search for stimulated desorption of neutral species. In the first, a quadrupole mass spectrometer was used to probe the ESD desorption products from the target. In the second, the desorbed species were probed indirectly by studying electron beam induced modifications to the irradiated surface with X-ray photoelectron spectroscopy (XPS).

2.1. High resolution quadrupole mass spectrometry

ESD experiments in which a high resolution quadrupole mass spectrometer (HRQMS) was employed as the desorption detector were conducted in a VG Scientific ESCALAB/SIMSLAB Mk.II ultra-high vacuum chamber with a 3×10^{-11} Torr base pressure. The vacuum chamber is actually composed of three chambers, each equipped with its own pumping facilities and separated from one another via gate valves. Typically, samples were mounted on stainless steel stubs, and admitted to the vacuum chamber (without venting and baking) by way of a fast-entry air-lock. A heatable, high pressure cell, located within the air-lock enables samples to be pretreated with various gases at elevated temperatures and pressures while the remainder of the system is maintained under UHV conditions. Following evacuation of the air-lock, the sample is transferred to the central chamber from where it may be shuttled along a rail system to either the XPS or SIMS chamber. This design allows several samples to be manipulated simultaneously, the result being that multiple samples may be analyzed, in succession, in a short period of time.

V_2O_5 powder (Aesar, 99.9%) and 0.127 mm thick V foil (Aldrich, 99.7%) were used to prepare the targets analyzed in this study. V_2O_5 pellets were formed in a laboratory press and further treated as indicated in Table 1. The high pressure cell was used for all the pellets listed in Table 1 except for the untreated pellet. The sintered pellet was transferred from the press to the sintering furnace and then retreated in the high pressure cell with O_2 at one atmosphere pressure. Following pretreatment in the high pressure cell, all targets were transferred, under vacuum, to the SIMS chamber to conduct ESD experiments. The V foil target was oxidized in a laboratory burner and then loaded into the vacuum chamber, bypassing the high pressure cell.

Table 1
Materials and methods used for the preparation of ESD targets

Material		Preparation method
V_2O_5 powder, 99.9%	pressed pellet	untreated
V_2O_5 powder, 99.9%	pressed pellet	heated to 550°C in 1 atm O_2
V_2O_5 powder, 99.9%	pressed pellet	sintered (625°C, 1 atm O_2, 12 h)
V_2O_5 powder, 99.9%	pressed pellet	H_2 reduction + ^{18}O oxidation
Vanadium foil, 99.7%	0.127 mm thick	flame oxidized

ESD experiments were carried out using either a standard Varian 981 series LEED/Auger electron gun (0.5–1 kV, 100 μA, $<$ 10 cm working distance) or a resistively heated W filament ($<$ 75 eV, $<$ 0.5 cm filament-to-sample distance). The desorption was detected using an Extrel C-50 high resolution quadrupole mass spectrometer. This unit was equipped with a high current electron bombardment ionizer and a six element ion optics system which comprises the ion source. The ionizer impact energy was calibrated against the ionization potential of argon gas. The quadrupole was operated at 2.1 MHz and was composed of rods measuring 1.9 cm in diameter and 22 cm in length. These features made it possible to achieve separation of signals derived from ^{16}O and CH_4 ($\simeq$ 0.03 amu). The output of a channeltron ion detector was fed to a pulse counting preamplifier whose output was signal averaged in a Tracor Northern TN-1750 multichannel analyzer.

2.2. X-ray photoelectron spectroscopy

An alternate approach to the investigation of the ESD process involves quantifying the target material changes that are induced through electron beam irradiation. An experiment of this type was conducted using XPS. Following preparation, a flame oxidized V foil target was characterized initially by XPS. The target was then transferred (under ultrahigh vacuum) to the SIMS chamber where it was subjected to 150 min of electron irradiation (850 V, 150 μA beam current) from the LEED/Auger electron gun. The target was then returned to the XPS chamber (still under ultrahigh vacuum) to record a post irradiation spectrum. The pressure in the two analytical chambers and the adjoining central chamber was $\leq 10^{-10}$ Torr during the course of the experiment. Mg Kα X-rays (1253.6 eV) were used as the surface probe, and the energy analyzer was operated at a constant 50 eV pass energy.

3. Results and discussion

3.1. High resolution quadrupole mass spectrometry

The main difficulty in detecting ESD O atoms with a mass spectrometer is identifying the source of the signal at mass 16. When the signal at mass 16 grows substantially relative to signals at all other masses during irradiation of the ESD target, then the increase in the mass 16 signal may be attributed to the ESD of atomic oxygen. Unfortunately, operation of the electron gun in our instrument produced increases in the signals at many masses, even at an operating pressure in the 10^{-11} Torr range, and even with the electron beam directed away from the ESD target. With significant, unwanted ESD from the vacuum chamber walls, it was unclear whether the increase at mass 16 was due to ESD O atoms or to methane. Although the CH_3^+/CH_4^+ signal ratio may be used to distinguish ^{16}O from CH_4 at a normal electron bombardment energy of 70 eV fragmentation of molecules containing oxygen such as CO, CO_2, or H_2O in the electron bombardment ionizer will also contribute to the signal at mass 16. The signal due to fragmentation can be reduced by lowering the mass spectrometer electron impact energy below the threshold for O^+ production from these molecules. However, there are a number of problems with this appearance potential approach. First, the appearance potential of CH_4^+ lies below the ionization potential of atomic oxygen so that there will always be a contribution to the signal at mass 16 from residual methane typically found in well-baked UHV chambers. Next, the fragmentation yield is very dependent on the electron impact energy so that the relative contribution to the mass 16 signal from methane and molecules containing oxygen changes as the ionizer electron impact energy is lowered. Thirdly, when the electron impact energy is below the threshold for CO_2 fragmentation, $\simeq 15$ eV, the lineshape and the signal-to-noise ratio deteriorate to the extent that positive identification of ESD O atoms is quite difficult. After attempting to conduct these experiments with two low resolution mass spectrometers (VG Masslab and UTI 100C) it was determined that truly unambiguous results may only be obtained from a high resolution instrument which provides both the total separation of ^{16}O from methane and maintains a good signal-to-noise ratio under the demanding conditions of low electron impact energies.

Fig. 1 shows a typical high resolution RGA spectrum collected with the Extrel QMS under UHV conditions. The spectrum is *not* the result of a gas backfill and demonstrates a signal-to-noise ratio obtained with minimal signal averaging. The absence

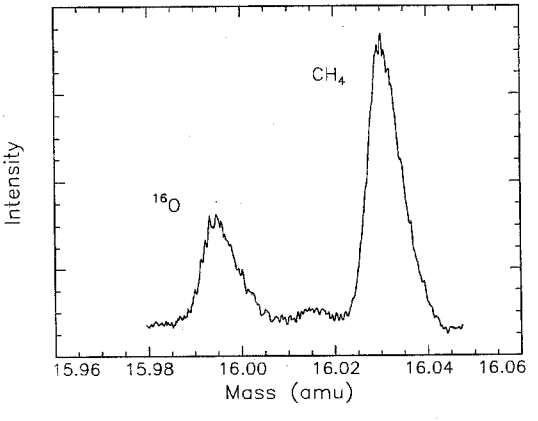

Fig. 1. High resolution mass spectrum collected with the Extrel C-50 QMS showing the completely resolved ^{16}O (15.995 amu) and CH_4 (16.013 amu) peaks.

of a flat baseline between the peaks is common in high resolution work and is generally described as a broadening of the main peak due to ions with excessive kinetic energy [24,25]. With ^{16}O and methane totally resolved, a change in either signal may now be unambiguously detected.

ESD spectra from an oxidized V foil target are shown in Fig. 2. With the target held at ground potential (Fig. 2a) so that ESD O^+ produced at the surface can be detected, the observed ^{16}O peak is broad and asymmetric, and it slopes to the low mass side. High resolution QMS peaks with these features are indicative of high energy species and are expected as ESD ions have been shown to possess several eV of kinetic energy (e.g. [4,9,15]). The origin of the ^{16}O peak is now identified by applying a target bias to suppress ion emission. By comparing the spectrum with the target at ground potential (Fig. 2a) to the spectrum measured with the target at -10 V (Fig. 2b), it is seen that the biggest contribution to the ^{16}O signal in Fig. 2a is ESD O^+. The QMS ionizer was on while both spectra were recorded. Similar results were obtained with the QMS ionizer off.

The source of the remaining neutral ^{16}O signal may now be investigated using the appearance potential technique. With the electron impact ionizer operating at a standard energy (70 eV), CO and CO_2 are likely candidates for ^{16}O interference, as these two species are generally the most abundant oxygen-containing gases in the residual atmosphere of a well-baked UHV chamber. As the impact energy is lowered, the large difference between the ionization potential of atomic oxygen ($\simeq$ 13.6 eV), and the O^+ appearance potential for either CO or CO_2 ($\simeq$ 23.6 and 19.5 eV respectively) [26] enables the ^{16}O source to be identified. By comparing the spectra in Fig. 3 (also from a V foil target), it is seen that the neutral ^{16}O signal that persists after ESD ion emission has been suppressed is produced from the electron impact induced fragmentation of CO in the ionizer; it is not ESD O^+ from the target.

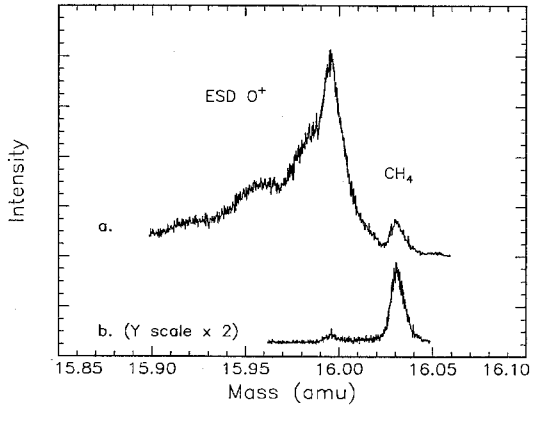

Fig. 2. ESD spectra from oxidized V demonstrating the effect of target bias. (a) Target bias = 0 V. (b) Target bias = -10 V.

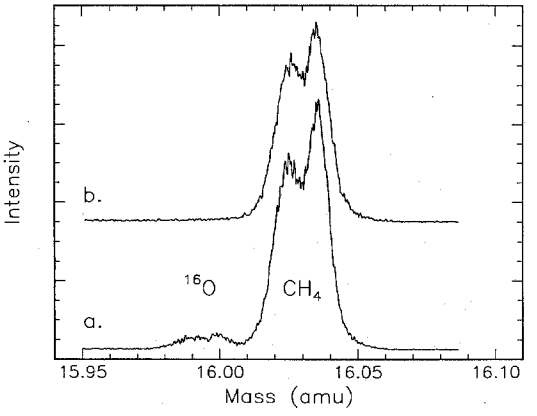

Fig. 3. Appearance potential analysis of the ^{16}O neutral fraction. (a) Electron impact energy = 70 eV. (b) Electron impact energy = 23 eV. The disappearance of the ^{16}O peak in (b) establishes its origin as CO.

A further contribution to the mass 16 signal may originate in the electron impact ionizer. Depending on the history of the QMS and the vacuum chamber, the impact of low energy electrons upon the walls of the ionizer or nearby surfaces can stimulate desorption of O^+, F^+, Cl^+, or other ions [27]. The significance of this interference is that these ions are generated at the ionizer and not the sample. Therefore, application of a bias voltage to the sample support or to an ion repelling grid positioned between the sample and the detector will not suppress this ion emission. In cases where the desired signal is much larger than the background this unavoidable ionizer ESD process is insignificant. However, for detection of ESD O atoms or other experiments characterized by a small signal on a larger back-

ground, this interference must be carefully addressed.

This type of ionizer interference was commonly observed in the last step of a typical experiment. In general, the experiments were conducted as follows: first, the QMS was tuned to resolve ^{16}O from CH_4. Next, a sample bias or ion repelling potential was established to suppress the ESD O^+ signal. The electron impact energy was then adjusted to discriminate between ESD O atoms and ^{16}O fragments from oxygen containing background gases. With ESD ions and background gas sources of ^{16}O eliminated from the spectrum, the remaining ^{16}O signal was generally reduced below one count per mass scan. At that point the spectrum was summed for hundreds (or thousands) of scans. Control experiments (gun on–gun off...) proved that what little signal was collected could not be attributed to the ESD of atomic oxygen.

While the only measurable contributions to apparent neutral ^{16}O peaks were CO fragmentation and O^+ produced in the ionizer, all of the preparation methods listed in Table 1 were found to produce ESD O^+. Fig. 2, discussed above, shows ESD ions from an oxidized V foil. ESD $^{16}O^+$ and $^{18}O^+$, desorbed from an $^{18}O_2$ treated V_2O_5 pellet (ionizer off, target at ground potential), are seen in Fig. 4. Even the untreated V_2O_5 pellet was found to produce ESD O^+. Several target preparation methods which include high temperature steps were employed (Table 1, entries 2 and 3) to determine whether water or other contamination could be responsible for the absence of an ESD O atom signal. The result was that the high temperature methods significantly minimized sample outgassing, but no ESD O atom signal was ever detected.

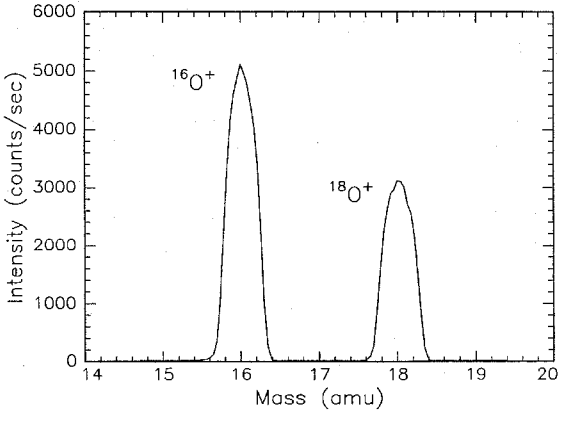

Fig. 4. ESD ion spectrum from a V_2O_5 pellet pretreated with $^{18}O_2$.

It is worth noting that although Table 1 lists only five entries, significantly more than five experiments were conducted which involved subtle changes in the preparation method (e.g. variations in preparation time, temperature or pressure). Likewise, the experiments were repeated using multiple measurement strategies including the use of different electron sources, irradiation of the target at different target temperatures, and changes in the method of ion rejection.

At this point, the ESD experiment is considered step by step, from the target surface to the desorption process to the detection method, to answer the question that follows naturally: Why was ESD atomic oxygen never detected? The first issue is that of target surface preparation. In general, surface cleanliness was considered to be a prerequisite to surface investigations and the state of cleanliness has nearly always been reported in the literature. However, in the case of stimulated desorption, there appears to be no reason, a priori, to expect that any of the surfaces investigated in this study should preferentially produce ionic species over neutrals. Accordingly, no effort was made to prepare scrupulously clean oxides. Rather the samples were prepared by which ever process was found to produce large ESD O^+ signals because the available information indicated that large ESD O^+ desorption yields are accompanied by larger ESD O atom desorption yields [4,14,15]. Nonetheless, surface cleanliness was monitored with XPS. Coincidently, the preparation methods used most often, sintering and flame oxidation, resulted in clean target surfaces. Comparison of the surfaces before and after preparation showed an obvious sharpening of the V and O features, a domination of the spectrum by the O(1s) and V(2p) peaks, and up to a ten-fold decrease in the surface C signal. Thus it does not appear that surface contamination explains the absence of atomic oxygen.

Another possible reason atomic oxygen was not detected could be that all desorbed O atoms were subsequently ionized in the ESD beam and detected as O^+. The fraction of ESD O atoms converted to

O^+ through electron impact ionization in the ESD electron beam can be calculated from

$$\frac{\Phi_{O^+}}{\Phi_O} = \Phi_e \frac{L}{v_O} \sigma_i, \quad (1)$$

where Φ_{O^+} is the O^+ flux produced through the electron impact ionization of O atoms, Φ_O is the flux of ESD O atoms desorbed from the target, Φ_e is the electron beam flux at the target, L is the length of the ionization region, v_O is the O atom velocity, and σ_i is the electron impact ionization cross-section. As written in Eq. (1), it is seen that the ratio, Φ_{O^+}/Φ_O, is dependent only on the electron beam flux, the ionization cross-section, and the O atom–electron beam interaction time, L/v_O. Φ_e is determined to be 2.07×10^{16} cm^{-2} s^{-1} from the electron beam current ($\simeq 100$ μA) and spot size ($\simeq 0.03$ cm^2). v_O is taken to be 7.7×10^5 cm s^{-1} based on reports of $\simeq 5$ eV O^+ desorbates [4,9,15]. L and σ_i, are determined from the experimental geometry and electron beam energy [28]. σ_i is $\simeq 8 \times 10^{-17}$ cm^2 and L is 0.14 cm. The calculated fraction of ESD O atoms converted to ESD O^+ through electron impact ionization in the ESD electron beam is 3×10^{-7}. Thus for the conditions typical of these experiments, the absence of detectable atomic oxygen cannot be due to ionization by the ESD electron beam.

Another question related to desorption, is the possibility that stimulated desorbates leave the surface molecularly, either as O_2 or another oxygen-containing molecule. That issue is best addressed with a mass balance type of experiment in which the extent of surface oxygen depletion is compared to the measured ESD O^+ yield. This is discussed in Section 3.2 below. It is noted, however, that during these experiments, ESD O_2 was never observed in accord with previous work on V_2O_5 [8].

The discussion now turns to the neutral detection sensitivity of the HRQMS. The HRQMS detection limit is calculated from a statistical analysis of the noise in baseline or 'blank' measurements following the convention adopted by the International Union of Pure and Applied Chemistry [29]. Specifically, a set of blank measurements was made under conditions that emulate the experiment in all manner except for the presence of the analyte. The limiting signal was then specified as the sum of the baseline average plus an integral number (k) of standard deviations. In the present calculation, $k = 3$ is used, to place the result within the 99.9% confidence limit. The limiting signal is then converted to the limiting concentration using the instrument response calibration curve. The result is a threshold density of 1.88×10^3 neutrals per cm^3. Based on reports of $\simeq 5$ eV ESD O^+ desorbates [4,9,15], the limiting density is expressed as 1.45×10^9 cm^{-2} s^{-1}, the flux of 5 eV ESD O atoms required to generate the limiting density.

Table 2
ESD results from three targets: included are the O^+ desorption rate from the target (yield), the corresponding O^+ flux (Φ), and the calculated neutral to ion ratio

Target	O^+ yield (counts/s)	Φ_{QMS,O^+} (O^+ cm^{-2} s^{-1})	O/O^+ ratio
Oxidized V foil	9.0×10^4	2.7×10^7	54
$^{18}O_2/V_2O_5$	8.3×10^4	2.5×10^7	58
V_2O_5 pellet	3.0×10^4	9.1×10^6	160

Given that ESD O atoms were not detected in this investigation, an upper limit of the ESD neutral to ion desorption ratio may be calculated by comparing the neutral detection threshold to the measured ESD O^+ yield. From Table 2, the ESD O^+ yield measured from oxidized V foil with the QMS ionizer off was 9.0×10^4 s^{-1}. This count rate is converted to the corresponding flux by including the quadrupole transmission factor and the aperture size. The result is an ESD O^+ flux at the QMS of 2.7×10^7 cm^{-2} s^{-1}. The resulting ratio of the neutral detection threshold to the measured ESD O^+ flux is $\simeq 54$. That is, from the calculated neutral detection sensitivity of the HRQMS for 5 eV ESD O atoms, the maximum number of ESD O atoms that could have been produced per ESD O^+ produced (from V foil) is roughly 50. The upper limit of the flux ratio from the other targets (Table 2) has been calculated in the same manner. It should be emphasized that the results shown in Table 2 are not intended as a comparison of the relative desorbate yields from different V oxides. Survey work requires that all experimental parameters, with the exception of preparation method, be reproduced exactly from experiment to experiment. The intention in this investigation was to produce neutral desorbates. Thus based on the available information which suggested that the neutral

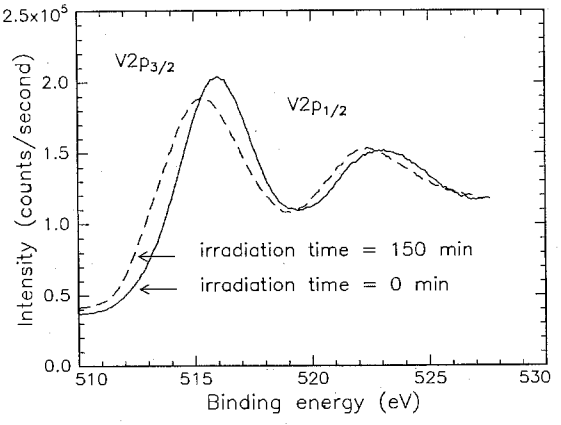

Fig. 5. V(2p) X-ray photoelectron spectrum showing the electron beam induced reduction of oxidized V. Solid curve = initial spectrum. Dashed curve = spectrum after 150 min of electron irradiation.

desorption yield followed the ionic desorption yield, every effort was made to maximize the ESD O^+ yield without strict regard to the reproduction of experimental conditions. As such, not all experiments were conducted at the same target temperature or electron beam current, etc. It is the case, however, that the search for ions and neutrals from a single sample was carried out under the same conditions.

3.2. ESD induced substrate changes: XPS

The experiments described thus far, have been limited to the detection and analysis of the products of the ESD process. Alternatively, the identity of the desorbing species may be inferred by monitoring the surface as it undergoes ESD induced change. In this section, XPS measurements of the electron beam induced surface modifications are presented.

Fig. 5 shows the changes in the V(2p) peaks resulting from the electron irradiation described in Section 2.2. Since the sample was shuttled from the XPS chamber to the SIMS chamber and back, and it may not have been returned to a position where the same location on the surface was analyzed by XPS, changes in the magnitude of the V peaks before (solid line) and after (dashed line) irradiation are not of importance here. Rather the quantity of interest is the change in the O/V peak ratios before and after irradiation. Following 2.5 h of irradiation this ratio was found to decrease by $\simeq 10\%$. (This change in ratios is not easily recognized by the eye and therefore the O peak has not been shown. The peak areas were determined through an integrating feature of the XPS software.)

The relationship between the number of oxygen species removed from the ESD target and the measured changes in the XPS signal may be calculated from

$$D = Cnk, \tag{2}$$

where D is the number of oxygen atoms depleted from the target per unit area, C is the O atom concentration before irradiation, per unit area per atomic layer, n is the number of atomic layers probed, and k is the fractional change in the XPS O signal. It should be noted that D represents the total number of oxygen species removed (per unit area) in any form.

If it is assumed that the target surface began as stoichiometric V_2O_5 prior to irradiation, then from the unit cell dimensions it may be seen that there are 1.22×10^{15} O atoms cm^{-2} with 4.37 Å between layers. The number of layers probed during the XPS experiment is related to the inelastic mean free path of the photoelectron, λ, which may be read from plots of the 'universal curve' [30]. The result is that the O(1s) signal is produced primarily in the top two atomic layers. Since the XPS signal decreased by 10%, the effect of 2.5 h of irradiation upon the oxidized V target, was the loss of 2.44×10^{14} O species per cm^2.

The measured oxygen depletion can be converted to an upper bound of the ESD O/O^+ ratio. The ESD O^+ count rate at the start of the experiment is typically 3.0×10^4 s^{-1}. Generally, in ESD experiments using a focused electron beam, the signal decay is seen to follow a $time^{-1/2}$ dependence for a continuous electron source [11]. The ESD signal corrected for the quadrupole transmission, solid angle factor, and electron beam spot size, corresponds to an initial flux of $\simeq 3.3 \times 10^{10}$ ESD O^+ cm^{-2} s^{-1}. Integrating over the irradiation period results in a total ESD O^+ loss of 6.4×10^{13} cm^{-2}. If it is now assumed that all unaccounted oxygen loss, as measured by the XPS, is attributable to O atom desorption, then the upper limit of the ESD O/O^+ ratio is $\simeq 4$.

4. Conclusion

The ESD O/O^+ ratio from V_2O_5 and oxidized V foil has been investigated with HRQMS and XPS to determine whether the ESD process necessarily liberates many neutral particles for every ionic particle, as is commonly accepted in the DIET field [10,31]. ESD neutral to ion ratios have been reported previously, however, the ratios were generally determined through investigations which relied upon indirect detection methods, and/or were limited to either substrate analysis or desorbate analysis. In the present study both direct and indirect methods were used and both ion and neutral yields were probed. Nonetheless, despite an extensive exploration of sample preparation methods and measurement variations, ESD O atoms were never detected despite the fact that ESD O^+ was detected from every sample. Accordingly, these findings are presented as an upper bound of the ESD O/O^+ ratio as determined from the neutral detection limit of the instrumental method used. From the QMS studies on oxidized V and $^{18}O_2/V_2O_5$, the ESD O/O^+ ratio was determined to be $\simeq 50$. The XPS results, from oxidized V, place the ratio at less than 10. Within the wide range of ESD ratios reported from gas dosed metal systems [14,15], the results of both the QMS and XPS studies consistently fall at the lower end. This is true even for the ESD O/O^+ ratio of 160 from V_2O_5 (Table 2). Furthermore, despite the possible shortcomings of the indirect detection methods discussed above, these results are consistent with those studies, particularly the ESD O/O^+ ratios of 49 and 55 from O_2/Mo [4] and ESD O/O^+ ratios of 10–20 from O_2/W [15,16].

It should be stressed that these values are *upper limits*. Thus despite the agreement between these results and the referenced results, it should be recognized from this study that the ESD O/O^+ ratio can be no larger than $\simeq 50$ and may be much smaller.

Acknowledgements

The authors gratefully acknowledge the support of the Air Force Office of Scientific Research. This work was funded through grant #AFOSR-91-0303.

References

[1] R.D. Ramsier and J.T. Yates, Jr., Surface Sci. Rep. 12 (1991) 246.
[2] N.H. Tolk, M.M. Traum, J.C. Tully and T.E. Madey, eds., Desorption Induced by Electronic Transitions (DIET I) (Springer, Berlin, 1983); W. Brenig and D. Menzel, eds., Desorption Induced by Electronic Transitions (DIET II) (Springer, Berlin, 1985); R.H. Stulen and M.L. Knotek, eds., Desorption Induced by Electronic Transitions (DIET III) (Springer, Berlin, 1988); G. Betz and P. Varga, eds., Desorption Induced by Electronic Transitions (DIET IV) (Springer, Berlin, 1990); A.R. Burns, E.B. Stechel and D.R. Jennison, eds., Desorption Induced by Electronic Transitions (DIET V) (Springer, Berlin, 1993).
[3] D. Menzel and R. Gomer, J. Chem. Phys. 41 (1964) 3311.
[4] P.A. Redhead, Can. J. Phys. 42 (1964) 886.
[5] M.L. Knotek and P.J. Feibelman, Phys. Rev. Lett. 40 (1978) 964.
[6] P.J. Feibelman and M.L. Knotek, Phys. Rev. B. 18 (1978) 6531.
[7] L. Fiermans and J. Vennik, Surf. Sci. 9 (1968) 187.
[8] M.N. Colpaert, P. Clauws, L. Fiermans and J. Vennik, Surf. Sci. 36 (1973) 513.
[9] J.F. van der Veen, F.J. Himpsel, D.E. Eastman and P. Heimann, Solid State Commun. 36 (1980) 99.
[10] H.J. Fan and L.D. Marks, Ultramicroscopy 31 (1989) 357.
[11] R. Ai, H.J. Fan, P.C. Stair and L.D. Marks, Mater. Res. Soc. Symp. Proc. 157 (1990) 599.
[12] R. Ai, H.J. Fan and L.D. Marks, Surf. Sci. 280 (1993) 369.
[13] L.D. Marks, V.A. Volpert and R. Ai, Surf. Sci. 280 (1993) 375.
[14] T.E. Madey and J.T. Yates, Jr., J. Vac. Sci. Technol. 8 (1971) 525.
[15] M. Nishijima and F.M. Propst, Phys. Rev. B 2 (1970) 2368.
[16] T.E. Madey and J.T. Yates, Jr., Surf Sci. 11 (1968) 327.
[17] P. Fuelner and D. Menzel, J. Vac. Sci. Technol. 17 (1980) 662.
[18] R.A. Outlaw, G.B. Hoflund and G.R. Corallo, Appl. Surf. Sci. 28 (1987) 235.
[19] M.D. Alvey, M.J. Dresser and J.T. Yates, Jr., Phys. Rev. Lett. 56 (1986) 367.
[20] N.H. Tolk, L.C. Feldman, J.S. Kraus, R.J. Morris, M.M. Traum and J.C. Tully, Phys. Rev. Lett. 46 (1981) 34.
[21] P.D. Johnson, X. Pan, J. Tranquada, S.L. Hulbert and E. Johnson, in: Desorption Induced by Electronic Transitions (DIET III), eds. R.H. Stulen and M.L. Knotek (Springer, Berlin, 1988).
[22] Ph. Avouris, R. Beigang, F. Boszo and R. Walkup, Chem. Phys. Lett. 129 (1986) 505.
[23] M. Jacoby, F.J. Northrup, P.C. Stair, E. Weitz and L.D. Marks, to be published.
[24] P.H. Dawson, Int. J. Mass Spectrom. Ion Phys. 14 (1974) 317.
[25] P.H. Dawson, Int. J. Mass Spectrom. Ion Phys. 17 (1975) 447.

[26] C.E. Moore, Atomic Energy Levels, Circular No. 467, Vol. 1 (National Bureau of Standards, 1949) p. 45.
[27] J.H. Batey, Vacuum 37 (1987) 659.
[28] L.J. Kieffer and G.H. Dunn, Rev. Mod. Phys. 38 (1966) 1.
[29] G.L. Long and J.D. Wineforder, Anal. Chem. 55 (1983) 712.
[30] D.P. Woodruff and T.A. Delchar, Modern Techniques of Surface Science (Cambridge University Press, Cambridge, 1986).
[31] T.E. Madey, J.T. Yates, Jr., D.A. King and C.J. Uhlaner, J. Chem. Phys. 52 (1970) 5215.